STATISTICS, OPTIMIZATION AND INFORMATION COMPUTING
*Stat., Optim. Inf. Comput.*, Vol. **x**, Month 2024, pp 0–13.
Published online in International Academic Press (www.IAPress.org)

# Optimal Placement and Sizing of PV Systems and D-STATCOMs in Medium-Voltage Distribution Networks Using the Atan-Sinc Optimization Algorithm

Oscar Danilo Montoya [1], Luis Fernando Grisales-Noreña [2], Rubén Iván Bolaños[3]

[1]*Grupo de Compatibilidad e Interferencia Electromagnética (GCEM), Facultad de Ingeniería, Universidad Distrital Francisco José de Caldas, Bogotá D.C. 110121, Colombia*
[2]*Grupo de Investigación en Alta Tensión—GRALTA, Escuela de Ingeniería Eléctrica y Electrónica, Universidad del Valle, Cali 760015, Colombia*
[3]*Facultad de Ingenierías, Instituto Tecnológico Metropolitano, Campus Robledo, Medellín 050036, Colombia.*

**Abstract** The integration of photovoltaic (PV) systems and D-STATCOMs into medium-voltage distribution networks shows significant potential for enhancing voltage profiles, minimizing power losses, and improving the overall system efficiency. This paper introduces the Atan-Sinc Optimization Algorithm (ASOA), a novel metaheuristic technique specifically designed for addressing the optimal placement and sizing of PV systems and D-STATCOMs. The ASOA leverages the unique mathematical properties of the functions $\mathrm{atan}\,(x)$ and $\mathrm{sinc}\,(x)$ to efficiently explore and exploit the solution space. To validate its effectiveness, a comprehensive comparative analysis was conducted against two state-of-the-art methods: the vortex search algorithm (VSA) and the sine cosine algorithm (SCA). The results demonstrate that the ASOA outperforms these benchmark techniques in terms of solution quality, convergence rate, and robustness. An economic metric confirms its superior capabilities in solving this complex optimization problem (with reductions of about $35.5429\%$ and $35.6707\%$ for 33- and 69-bus grids, respectively). This research highlights the ASOA as a promising tool for enhancing the planning and operation of distribution networks, laying a strong foundation for future applications in power system optimization.

**Keywords** Atan-Sinc Optimization Algorithm (ASOA); Photovoltaic plants (PV); Distribution Static Compensators (D-STATCOM); Master-Slave Optimization

**AMS 2010 subject classifications** 62J07

**DOI:**10.19139/soic-2310-5070-2164

## 1. Introduction

### *1.1. General context*

The need for energy-efficient electrical networks has grown significantly in response to increasing global energy demand and the transition toward sustainable development [1]. As modern power systems evolve, enhancing the efficiency of electrical distribution networks has become essential for reducing energy losses, improving voltage stability, and ensuring reliable service delivery [2]. Distribution networks, which account for a substantial share of total energy losses, represent a critical area for optimization [3, 4]. Addressing these inefficiencies not only supports the delivery of electricity with minimal waste but also ensures the grid's ability to meet rising

*Correspondence to: O. D. Montoya (Email: odmontoyag@udistrital.edu.co). Facultad de Ingeniería, Universidad Distrital Francisco José de Caldas, Bogotá D.C. 110121, Colombia.

ISSN 2310-5070 (online) ISSN 2311-004X (print)

consumption in urbanized regions [5]. Integrating renewable energy technologies, particularly photovoltaic (PV) systems, has proven to be a viable solution for achieving these objectives while aligning with global efforts to mitigate environmental impacts [6, 7].

The deployment of PV systems in distribution grids provides dual benefits: reduced greenhouse gas emissions and enhanced grid efficiency through the utilization of clean solar energy [8, 9]. However, the effectiveness of PV systems can be significantly amplified by incorporating reactive power compensators such as D-STATCOMs. This combination leverages the active power generation of PV systems and the reactive power support of compensators to enhance voltage profiles, minimize energy losses, and the improve overall grid reliability [10]. Consequently, the coordinated integration of PV systems and D-STATCOMs emerges as a strategic approach for advancing energy-efficient and sustainable power distribution networks [11]. Figure 1 illustrates the installation process of a set of PV plants and D-STATCOMs within a distribution grid.


Figure 1. Illustration of a distribution company workgroup installing PV systems and D-STATCOMs in a medium-voltage distribution network

### *1.2. Motivation*

While numerous studies have explored the integration of PV systems and D-STATCOMs in distribution networks, evolving energy demands and the increasing penetration of renewable energy call for more advanced optimization techniques [11]. The interplay between active and reactive power flow in grids with significant distributed generation introduces complex operational challenges, particularly concerning voltage stability and power quality [12]. Existing research has highlighted the importance of optimizing the placement and sizing of PV systems and reactive power compensators to achieve cost-effective and technically sound solutions [13]. However, some gaps remain regarding the development of efficient algorithms that can address the highly nonlinear and combinatorial nature of these optimization problems [10].

Recent advancements in metaheuristic optimization have provided promising tools for addressing these challenges. Algorithms such as the Atan-Sinc Optimization Algorithm (ASOA) can efficiently navigate high-dimensional search spaces while balancing exploration and exploitation. The ASOA, inspired by the mathematical

properties of the arctangent and sinc functions, has shown potential in solving complex energy optimization problems with improved accuracy and computational efficiency [14, 15]. By leveraging the ASOA's unique characteristics, this study aims to develop a robust framework for the optimal integration of PV systems and D-STATCOMs that ensures enhanced grid performance while meeting sustainability targets.

### *1.3. Literature review*

Research on the integration of PV systems and D-STATCOMs in medium-voltage distribution networks has extensively focused on optimizing their placement and sizing to minimize energy losses and improve voltage profiles. Various optimization methods such as the Vortex Search Algorithm (VSA), the Sine-Cosine Algorithm (SCA), Multi-Verse Optimization (MVO), and the Generalized Normal Distribution Optimizer (GNDO), have been proposed to tackle these challenges. For instance, [10] demonstrated the effectiveness of the VSA in reducing long-term operating costs. Meanwhile, [16] highlighted the advantages of the SCA in achieving superior optimization results, outperforming the VSA in various scenarios. Furthermore, hybrid approaches that combine analytical techniques with metaheuristic algorithms have shown promise in addressing the complexity of optimization problems related to distribution networks [17, 18].

In addition to conventional optimization strategies, PV-STATCOMs have gained attention for their ability to enhance power quality and grid stability. Studies such as [19] and [20] have demonstrated the potential of these devices to mitigate harmonic distortions, stabilize voltage, and improve system reliability under dynamic load and solar conditions. These advancements underscore the growing importance of integrating advanced optimization techniques and innovative technologies in modern power systems.

### *1.4. Contributions and scope*

This research proposes a novel master-slave optimization framework based on the ASOA for the optimal placement and sizing of PV systems and D-STATCOMs in medium-voltage distribution networks. Here, the master stage employs the ASOA to determine the optimal configuration for PV and D-STATCOM devices, utilizing a hybrid discrete-continuous encoding scheme. The slave stage implements a successive approximations power flow algorithm to validate the technical feasibility of the solutions and ensure compliance with operational constraints. The effectiveness of this ASOA approach is demonstrated through numerical evaluations on benchmark distribution networks, including 33-bus and 69-bus test systems.

The scope of this study encompasses the integration of real-world demand and solar generation profiles, enabling an accurate representation of daily operational conditions [11]. The proposed methodology was benchmarked against existing optimization techniques, such as the VSA and SCA, in order to highlight its superiority in terms of cost minimization and solution quality [10, 16]. The findings provide valuable insights into the practical implementation of advanced optimization frameworks for enhancing the performance and sustainability of electrical distribution networks.

### *1.5. Document structure*

The remainder of this document is organized as follows. Section 2 introduces the mathematical formulation of the optimization model for PV and D-STATCOM device integration, including the objective function and the constraints involved. Section 3 presents the proposed solution methodology, detailing the application of the ASOA within the master-slave framework. Section 4 describes the test cases, including the network parameters, operational constraints, and solar generation profiles. Section 5 discusses the computational results and compares the proposed approach against existing methods. Finally, Section 6 summarizes the key findings and suggests future research directions.

## 2. Mathematical model for an optimal PV and D-STATCOM integration

This section provides the mathematical formulation for the optimal placement and sizing of PV systems and D-STATCOMs in medium-voltage distribution networks. The problem is structured as a mixed-integer nonlinear programming (MINLP) model, encompassing an objective function and a set of constraints that ensure technical and operational feasibility [11].

### *2.1. Objective function*

The goal is to minimize the total costs associated with energy purchase, investments made in PV systems, and maintenance expenses [16]. The objective function is expressed as follows:

$$\min z_{\text{cost}} = z_1 + z_2, \tag{1}$$

where:

- $z_1$: Total energy purchase cost, calculated as

$$z_1 = C_{kWh} T f_a f_c \sum_{h\in\mathcal{H}} \sum_{i\in\mathcal{N}} p^{cg}_{i,h} \Delta h, \tag{2}$$

  where:

  – $C_{kWh}$: Cost of energy per kWh
  – $T$: Considered time period
  – $f_a$: Annualization factor
  – $f_c$: Cost adjustment factor for inflation
  – $\mathcal{H}$: Set of time intervals in a day
  – $\mathcal{N}$: Set of buses in the distribution network
  – $p^{cg}_{i,h}$: Power supplied by the conventional generator at bus $i$ during time $h$ (kW)
  – $\Delta h$: Duration of each time interval (hours)

- $z_2$: Investment and maintenance costs, expressed as:

$$z_2 = C_{pv} f_a \sum_{i\in\mathcal{N}} p^{pv}_i + T \sum_{h\in\mathcal{H}} \sum_{i\in\mathcal{N}} C^{pv}_{O\&M} p^{pv}_{i,h} \Delta h + \gamma \sum_{i\in\mathcal{N}} \left(\omega_1 ({q_i}^{comp})^2 + \omega_2 {q_i}^{comp} + \omega_3\right) q^{comp}_i, \tag{3}$$

  where:

  – $C_{pv}$: Investment cost per unit of PV capacity (currency/kW)
  – $p^{pv}_i$: PV capacity installed at bus $i$ (kW)
  – $C^{pv}_{O\&M}$: Operation and maintenance cost of PV systems per kWh
  – $p^{pv}_{i,h}$: Power generated by the PV system at bus $i$ during time $h$ (kW)
  – $\gamma$: Weighting factor for the cost of reactive power compensation
  – $q^{comp}_i$: Reactive power compensation at bus $i$ (kvar)
  – $\omega_1, \omega_2, \omega_3$: Coefficients for the cost model of the compensators

### *2.2. Constraints*

The model includes several constraints to ensure system reliability and feasibility.

*2.2.1. Power flow equations* The active and reactive power balance equations for each bus $i$ are as follows [10]:

$$p^{cg}_{i,h} + p^{pv}_{i,h} - P^d_{i,h} = v_{i,h} \sum_{j\in\mathcal{N}} Y_{ij} v_{j,h} \cos(\theta_{i,h} - \theta_{j,h} - \varphi_{ij}), \qquad \{\forall i \in \mathcal{N},\ \forall h \in \mathcal{H}\} \tag{4}$$

$$q^{cg}_{i,h} + q^{comp}_{i,h} - Q^d_{i,h} = v_{i,h} \sum_{j\in\mathcal{N}} Y_{ij} v_{j,h} \sin(\theta_{i,h} - \theta_{j,h} - \varphi_{ij}). \qquad \{\forall i \in \mathcal{N},\ \forall h \in \mathcal{H}\} \tag{5}$$

where:

- $P_{i,h}^{d}$, $Q_{i,h}^{d}$: Active and reactive power demand at bus $i$ during time $h$ (kW and kvar)
- $v_{i,h}, \theta_{i,h}$: Voltage magnitude and angle at bus $i$ during time $h$ (V and radians)
- $Y_{ij}$: Admittance of the line between buses $i$ and $j$ (S)
- $\varphi_{ij}$: Phase angle of the admittance $Y_{ij}$ (radians)

*2.2.2. Power generation bounds* The generation limits are defined as follows [16]:

$$P_i^{cg,\min} \leq p_{i,h}^{cg} \leq P_i^{cg,\max}, \qquad \{\forall i \in \mathcal{N},\ \forall h \in \mathcal{H}\} \tag{6}$$

$$Q_i^{cg,\min} \leq q_{i,h}^{cg} \leq Q_i^{cg,\max}, \qquad \{\forall i \in \mathcal{N},\ \forall h \in \mathcal{H}\} \tag{7}$$

$$x_i^{pv} P_i^{pv,\min} \leq p_i^{pv} \leq x_i^{pv} P_i^{pv,\max}, \qquad \{\forall i \in \mathcal{N}\} \tag{8}$$

$$p_{i,h}^{pv} = G_{i,h}^{pv} p_i^{pv}. \qquad \{\forall i \in \mathcal{N},\ \forall h \in \mathcal{H}\} \tag{9}$$

where:

- $P_i^{cg,\min}$, $P_i^{cg,\max}$: Minimum and maximum limits for the active power output of the conventional generator at bus $i$ during time $h$ (kW)
- $Q_i^{cg,\min}$, $Q_i^{cg,\max}$: Minimum and maximum limits for the reactive power output of the conventional generator at bus $i$ during time $h$ (kvar)
- $P_{i,h}^{pv,\min}$, $P_{i,h}^{pv,\max}$: Minimum and maximum limits for the active power output of the PV source at bus $i$ during time $h$ (kW)
- $G_{i,h}^{pv}$: Solar generation availability factor at bus $i$ during time $h$ (%)

*2.2.3. Voltage regulation* The voltage at each bus must remain within acceptable operational limits [21]:

$$v^{\min} \leq v_{i,h} \leq v^{\max}. \qquad \{\forall i \in \mathcal{N},\ \forall h \in \mathcal{H}\} \tag{10}$$

where:

- $v^{\min}$, $v^{\max}$: Minimum and maximum limits associated with the voltage regulation at each node (V)

*2.2.4. Device installation constraints* These constraints govern the installation of PV systems and compensators:

$$\sum_{i \in \mathcal{N}} x_i^{pv} \leq N_{pv}^{ava}, \tag{11}$$

$$x_i^{comp} Q_i^{comp,\min} \leq q_i^{comp} \leq x_i^{comp} Q_i^{comp,\max}, \qquad \{\forall i \in \mathcal{N}\} \tag{12}$$

$$q_{i,h}^{comp} = q_i^{comp}, \qquad \{\forall i \in \mathcal{N},\ \forall h \in \mathcal{H}\} \tag{13}$$

$$\sum_{i \in \mathcal{N}} x_i^{comp} \leq N_{comp}^{ava}. \tag{14}$$

where:

- $N_{pv}^{ava}$, $N_{comp}^{ava}$: Maximum number of PV systems and compensators allowed in the network
- $x_i^{pv}$, $x_i^{comp}$: Binary variables indicating the presence of PV systems or compensators at bus $i$

*2.2.5. Annualization and energy costs* The annualization factor $f_a$ and the energy cost adjustment factor $f_c$ are calculated as follows [11]:

$$f_a = \frac{t_a}{1 - (1 + t_a)^{-N_t}}, \tag{15}$$

$$f_c = \sum_{t \in \mathcal{T}} \left( \frac{1 + t_e}{1 + t_a} \right)^t. \tag{16}$$

where:

- $t_a$: Annual discount rate
- $t_e$: Annual energy inflation rate
- $N_t$: Project lifespan (years)
- $\mathcal{T}$: Set of years within the project horizon

### *2.3. Model characteristics*

The unified mathematical model encompasses non-convex, convex, and binary components, highlighting the complexity of the optimization problem [11]. Table 1 categorizes and details these components.

Table 1. Classification of model components in the unified optimization framework

| **Component type** | **Description and characteristics** |
|---|---|
| **Non-convex components** | The objective function (1) and the Equality Constraints (4) and (5) exhibit nonlinear and non-convex properties due to the inclusion of trigonometric sine and cosine terms, voltage-variable interactions, and cubic expressions. These components contribute to the complexity of the optimization problem. |
| **Convex components** | This subset includes linear and convex constraints, such as the Inequality Constraints (6), (7), and (10) and the Equality Constraints (9) and (13). These elements primarily establish upper and lower bounds for decision variables, ensuring feasibility and operational reliability. |
| **Binary components** | The Binary Constraints (8), (11), (12), and (14) involve discrete decision variables. These variables determine specific actions, such as installing (or not) PV systems or D-STATCOMs at particular locations in the network. |
| **Excluded components** | Equations (15) and (16) are not classified in the above-presented categories. Instead, they define constant parameters related to annualization and projected energy costs over the project's duration. |

## 3. Solution strategy

The optimization problem defined by Equations (1)–(14) is addressed using a two-stage approach. In the first stage, referred to as the *master stage*, the ASOA is used to determine the optimal locations and capacities of the PV systems and the D-STATCOMs. Once these decision variables have been optimized, they move on to the second stage, known as the *slave stage*. Here, a power flow algorithm specifically designed for distribution networks is employed to verify the feasibility of the solution [22]. This validation step ensures that the power balance constraints are met and provides a comprehensive evaluation of voltage profiles and power generation for each scenario. The next sections detail the key components of this solution approach.

### *3.1. Master stage: the Atan-Sinc Optimization Algorithm*

This subsection presents the adaptation of the ASOA for solving optimization problems with equality and inequality constraints using a penalty-based approach. The proposed implementation allows this algorithm to effectively manage complex constraints by transforming the original constrained problem into an unconstrained one, applying penalties to ensure solution feasibility.

*3.1.1. Algorithm inspiration* ASOA is a population-based metaheuristic optimization technique inspired by the mathematical properties of the arctangent and sinc functions [23, 24], *i.e.*,

$$f(x) = \frac{2}{\pi}\text{atan}(\pi x),$$
$$g(x) = \frac{1}{\pi x}\text{sinc}(\pi x).$$

Figure 2, presents the graphical behavior of both functions. Note that these functions have complementary characteristics that make them well-suited for optimization tasks. The arctangent function ensures controlled and smooth movements near optimal solutions, enhancing local exploitation, while the oscillatory behavior of the sinc function facilitates the global exploration of the search space. This balance helps the algorithm to avoid stagnation in local optima and achieve efficient convergence towards the global solution.

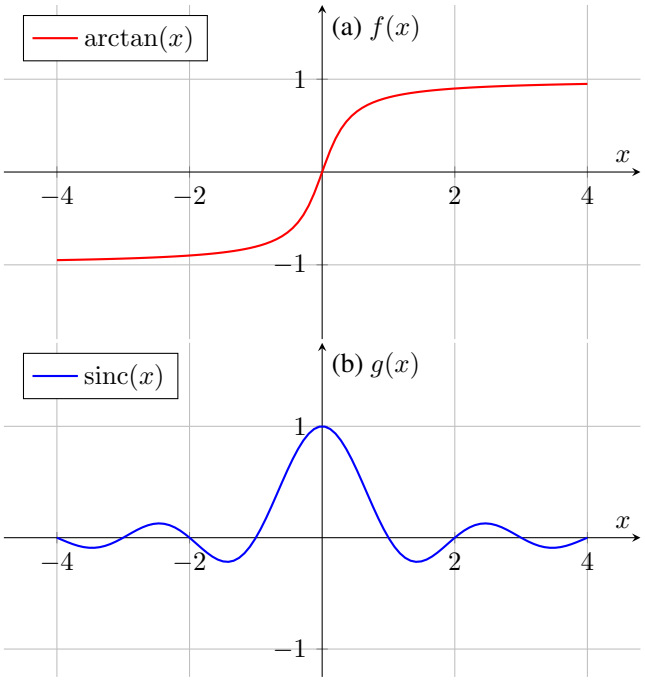


Figure 2. Graphical representation of the atan$(x)$ and sinc$(x)$ functions: (a) atan$(x)$, and (b) sinc$(x)$

The ASOA is capable of addressing both continuous and discrete optimization problems. Its adaptability makes it a robust and versatile tool applicable in fields such as energy planning, structural design, and resource management. However, like other metaheuristic algorithms, its direct application to constrained problems is limited. To address this limitation, a penalty scheme is used to transform the constrained problem into an unconstrained one, guiding solutions toward feasibility.

*3.1.2. Adapting the ASOA* The adaptation of the ASOA employs a penalty function $P(x)$, transforming the constrained problem into [25]

$$\min_{x\in\mathbb{R}^n} F(x) = f(x) + P(x). \tag{17}$$

*3.1.3. Initial population and penalized objective function evaluation* The algorithm generates an initial population $X^t$ of candidate solutions within the search space. Each solution is evaluated using $F(x)$, and the best solution is

selected as follows [25]:

$$x_{\text{best}}^{t} = \arg\min_{k} F(x_k^t), \quad \forall k = 1, 2, \ldots, n_s. \tag{18}$$

The proposed encoding approach represents the decision variables for the optimal placement and sizing of PV systems and D-STATCOMs in a distribution network. Below is a detailed breakdown of its structure, interpretation, and implications for the optimization process.

The decision variables include:

- The bus locations for PVs and D-STATCOMs.
- The capacities of each installed component.

For a distribution network with 33 nodes, the encoding of a candidate solution is structured as follows:

$$x_k^t = \begin{bmatrix} 5 & 16 & 21 & 33 & 532.32 & 1650.50 & 722.20 & 1001.40 \end{bmatrix} \tag{19}$$

where:

- The first four elements $\{5, 16, 21, 33\}$ represent the bus locations of two PVs and two D-STATCOMs.
- The last four elements $\{532.32, 1650.50, 722.20, 1001.40\}$ indicate their respective nominal capacities in kW and kvar.

*3.1.4. Updating the rules and generating new solutions* The ASOA utilizes the functions $((2/\pi)\text{atan}(\pi r_2))$ and $((1/\pi)\sin(\pi r_2)/r_2)$ to generate new solutions, dynamically adjusting exploration and exploitation behaviors based on the properties of these functions [16]. The update rules are defined as follows:

$$y_k^t = \begin{cases} x_k^t + \frac{2r_1}{\pi}\text{atan}(\pi r_2) \cdot |r_3 x_{\text{best}}^t - (1 - r_3)\, x_k^t| & r_4 \leq 0.5, \\ x_k^t + \frac{r_1}{\pi}\frac{\sin(\pi r_2)}{r_2} \cdot (r_3 x_{\text{best}}^t - (1 - r_3)\, x_k^t) & r_4 > 0.5, \end{cases} \tag{20}$$

where $r_2, r_3, r_4$ are random parameters dynamically generated in each iteration, and $r_1$ defines an exponential decreasing rule that balances the exploration and exploitation of the solution space. Mathematically, $r_1$ is defined as follows:

$$r_1 = 2\left(1 - \frac{t}{t_{\max}}\right)\exp\left(-2\frac{t}{t_{\max}}\right).$$

The arctangent function in (20) ensures controlled movements within a finite range, ideal for local exploitation, while the sinc function's oscillatory behavior allows for a broad coverage of the search space, promoting effective global exploration. The parameter $r_2$ is randomly sampled within $[-4, 4]$, ensuring sufficient diversity.

*3.1.5. Solution correction and penalty application* The generated solutions $y_k^t$ are adjusted to respect the problem's bounds, with projection rules applied when necessary in order to ensure feasibility within the search space.

*3.1.6. Replacement and stopping criteria* The solutions generated are compared to the current ones and replaced according to [26]:

$$x_k^t = \begin{cases} y_k^t & \text{if } F(y_k^t) < F(x_k^t), \\ x_k^t & \text{otherwise.} \end{cases} \tag{21}$$

The algorithm terminates either upon reaching a maximum number of iterations or when no significant improvements are observed over a predefined number of consecutive iterations.

## 4. Test feeders and model characterization

### *4.1. Hybrid optimization approach and test systems*

The hybrid master-slave optimization strategy integrates the ASOA with the successive approximations power flow technique. This methodology was utilized to determine the optimal placement and sizing of PV systems and D-STATCOMs in distribution networks. The key details are summarized below:

- **Optimization strategy:** The hybrid master-slave approach combines:
  - **A master layer:** The ASOA, in order to explore and determine the best configuration for the PV systems and D-STATCOMs.
  - **A slave layer:** The successive approximations power flow technique, in order to validate the feasibility of candidate solutions.
- **Test systems:**
  - **Benchmark networks:** 33-bus and 69-bus radial test feeders.
  - **Voltage levels:** Nominal voltage of 12,660 V at the substation.
  - **Voltage constraints:** Operation within a permissible range of $\pm 10\%$.

The electrical layouts of the test systems are depicted in Figure 3, and their main characteristics are presented in Table 3.

Table 2. Electrical characteristics of the benchmark test feeders

| Test system | Number of buses | Total load (kW/kvar) | Nominal voltage (V) |
|---|---|---|---|
| 33-bus | 33 | 3,715 / 2,300 | 12,660 |
| 69-bus | 69 | 3,802 / 2,694 | 12,660 |

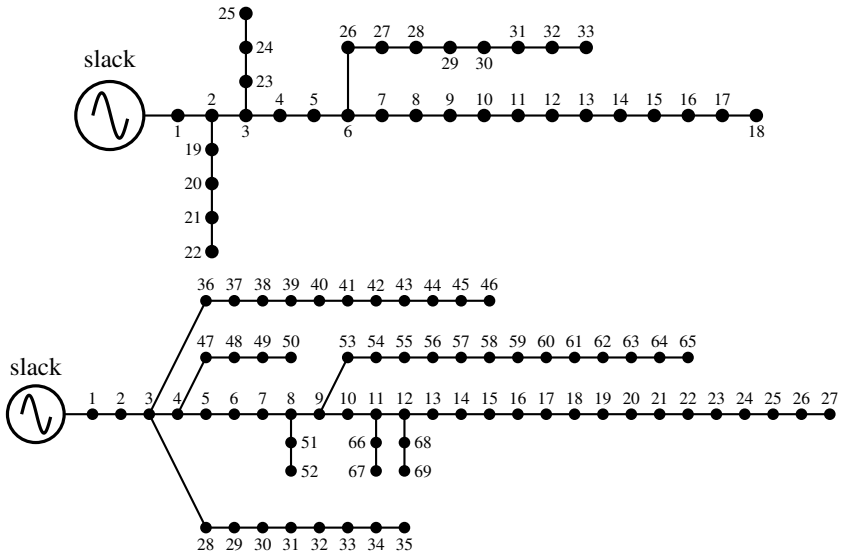


Figure 3. Single-line diagrams of the 33- and 69-bus distribution systems

The performance of the proposed methodology for determining the optimal placement and capacity of PV systems and D-STATCOMs in medium-voltage distribution networks was assessed by incorporating projected

Table 3. Branch and load data for the 33- and 69-bus grids

| 33-bus grid | | | | | | | | | | | |
|---|---|---|---|---|---|---|---|---|---|---|---|
| **Node $i$** | **Node $j$** | **$R_{ij}$ (Ω)** | **$X_{ij}$ (Ω)** | **$P_j$ (kW)** | **$Q_j$ (kvar)** | **Node $i$** | **Node $j$** | **$R_{ij}$ (Ω)** | **$X_{ij}$ (Ω)** | **$P_j$ (kW)** | **$Q_j$ (kvar)** |
| 1 | 2 | 0.0922 | 0.0477 | 100 | 60 | 17 | 18 | 0.7320 | 0.5740 | 90 | 40 |
| 2 | 3 | 0.4930 | 0.2511 | 90 | 40 | 2 | 19 | 0.1640 | 0.1565 | 90 | 40 |
| 3 | 4 | 0.3660 | 0.1864 | 120 | 80 | 19 | 20 | 1.5042 | 1.3554 | 90 | 40 |
| 4 | 5 | 0.3811 | 0.1941 | 60 | 30 | 20 | 21 | 0.4095 | 0.4784 | 90 | 40 |
| 5 | 6 | 0.8190 | 0.7070 | 60 | 20 | 21 | 22 | 0.7089 | 0.9373 | 90 | 40 |
| 6 | 7 | 0.1872 | 0.6188 | 200 | 100 | 3 | 23 | 0.4512 | 0.3083 | 90 | 50 |
| 7 | 8 | 1.7114 | 1.2351 | 200 | 100 | 23 | 24 | 0.8980 | 0.7091 | 420 | 200 |
| 8 | 9 | 1.0300 | 0.7400 | 60 | 20 | 24 | 25 | 0.8960 | 0.7011 | 420 | 200 |
| 9 | 10 | 1.0400 | 0.7400 | 60 | 20 | 6 | 26 | 0.2030 | 0.1034 | 60 | 25 |
| 10 | 11 | 0.1966 | 0.0650 | 45 | 30 | 26 | 27 | 0.2842 | 0.1447 | 60 | 25 |
| 11 | 12 | 0.3744 | 0.1238 | 60 | 35 | 27 | 28 | 1.0590 | 0.9337 | 60 | 20 |
| 12 | 13 | 1.4680 | 1.1550 | 60 | 35 | 28 | 29 | 0.8042 | 0.7006 | 120 | 70 |
| 13 | 14 | 0.5416 | 0.7129 | 120 | 80 | 29 | 30 | 0.5075 | 0.2585 | 200 | 600 |
| 14 | 15 | 0.5910 | 0.5260 | 60 | 10 | 30 | 31 | 0.9744 | 0.9630 | 150 | 70 |
| 15 | 16 | 0.7463 | 0.5450 | 60 | 20 | 31 | 32 | 0.3105 | 0.3619 | 210 | 100 |
| 16 | 17 | 1.2860 | 1.7210 | 60 | 20 | 32 | 33 | 0.3410 | 0.5302 | 60 | 40 |
| 69-bus grid | | | | | | | | | | | |
| **Node $i$** | **Node $j$** | **$R_{ij}$ (Ω)** | **$X_{ij}$ (Ω)** | **$P_j$ (kW)** | **$Q_j$ (kvar)** | **Node $i$** | **Node $j$** | **$R_{ij}$ (Ω)** | **$X_{ij}$ (Ω)** | **$P_j$ (kW)** | **$Q_j$ (kvar)** |
| 1 | 2 | 0.0005 | 0.0012 | 0.00 | 0.00 | 3 | 36 | 0.0044 | 0.0108 | 26.00 | 18.55 |
| 2 | 3 | 0.0005 | 0.0012 | 0.00 | 0.00 | 36 | 37 | 0.0640 | 0.1565 | 26.00 | 18.55 |
| 3 | 4 | 0.0015 | 0.0036 | 0.00 | 0.00 | 37 | 38 | 0.1053 | 0.1230 | 0.00 | 0.00 |
| 4 | 5 | 0.0251 | 0.0294 | 0.00 | 0.00 | 38 | 39 | 0.0304 | 0.0355 | 24.00 | 17.00 |
| 5 | 6 | 0.3660 | 0.1864 | 2.60 | 2.20 | 39 | 40 | 0.0018 | 0.0021 | 24.00 | 17.00 |
| 6 | 7 | 0.3810 | 0.1941 | 40.40 | 30.00 | 40 | 41 | 0.7283 | 0.8509 | 1.20 | 1.00 |
| 7 | 8 | 0.0922 | 0.0470 | 75.00 | 54.00 | 41 | 42 | 0.3100 | 0.3623 | 0.00 | 0.00 |
| 8 | 9 | 0.0493 | 0.0251 | 30.00 | 22.00 | 42 | 43 | 0.0410 | 0.0478 | 6.00 | 4.30 |
| 9 | 10 | 0.8190 | 0.2707 | 28.00 | 19.00 | 43 | 44 | 0.0092 | 0.0116 | 0.00 | 0.00 |
| 10 | 11 | 0.1872 | 0.0619 | 145.00 | 104.00 | 44 | 45 | 0.1089 | 0.1373 | 39.22 | 26.30 |
| 11 | 12 | 0.7114 | 0.2351 | 145.00 | 104.00 | 45 | 46 | 0.0009 | 0.0012 | 29.22 | 26.30 |
| 12 | 13 | 1.0300 | 0.3400 | 8.00 | 5.00 | 4 | 47 | 0.0034 | 0.0084 | 0.00 | 0.00 |
| 13 | 14 | 1.0440 | 0.3450 | 8.00 | 5.50 | 47 | 48 | 0.0851 | 0.2083 | 79.00 | 56.40 |
| 14 | 15 | 1.0580 | 0.3496 | 0.00 | 0.00 | 48 | 49 | 0.2898 | 0.7091 | 384.70 | 274.50 |
| 15 | 16 | 0.1966 | 0.0650 | 45.50 | 30.00 | 49 | 50 | 0.0822 | 0.2011 | 384.70 | 274.50 |
| 16 | 17 | 0.3744 | 0.1238 | 60.00 | 35.00 | 8 | 51 | 0.0928 | 0.0473 | 40.50 | 28.30 |
| 17 | 18 | 0.0047 | 0.0016 | 60.00 | 35.00 | 51 | 52 | 0.3319 | 0.1114 | 3.60 | 2.70 |
| 18 | 19 | 0.3276 | 0.1083 | 0.00 | 0.00 | 9 | 53 | 0.1740 | 0.0886 | 4.35 | 3.50 |
| 19 | 20 | 0.2106 | 0.0690 | 1.00 | 0.60 | 53 | 54 | 0.2030 | 0.1034 | 26.40 | 19.00 |
| 20 | 21 | 0.3416 | 0.1129 | 114.00 | 81.00 | 54 | 55 | 0.2842 | 0.1447 | 24.00 | 17.20 |
| 21 | 22 | 0.0140 | 0.0046 | 5.00 | 3.50 | 55 | 56 | 0.2813 | 0.1433 | 0.00 | 0.00 |
| 22 | 23 | 0.1591 | 0.0526 | 0.00 | 0.00 | 56 | 57 | 1.5900 | 0.5337 | 0.00 | 0.00 |
| 23 | 24 | 0.3463 | 0.1145 | 28.00 | 20.00 | 57 | 58 | 0.7837 | 0.2630 | 0.00 | 0.00 |
| 24 | 25 | 0.7488 | 0.2475 | 0.00 | 0.00 | 58 | 59 | 0.3042 | 0.1006 | 100.00 | 72.00 |
| 25 | 26 | 0.3089 | 0.1021 | 14.00 | 10.00 | 59 | 60 | 0.3861 | 0.1172 | 0.00 | 0.00 |
| 26 | 27 | 0.1732 | 0.0572 | 14.00 | 10.00 | 60 | 61 | 0.5075 | 0.2585 | 1244.00 | 888.00 |
| 3 | 28 | 0.0044 | 0.0108 | 26.00 | 18.60 | 61 | 62 | 0.0974 | 0.0496 | 32.00 | 23.00 |
| 28 | 29 | 0.0640 | 0.1565 | 26.00 | 18.60 | 62 | 63 | 0.1450 | 0.0738 | 0.00 | 0.00 |
| 29 | 30 | 0.3978 | 0.1315 | 0.00 | 0.00 | 63 | 64 | 0.7105 | 0.3619 | 227.00 | 162.00 |
| 30 | 31 | 0.0702 | 0.0232 | 0.00 | 0.00 | 64 | 65 | 1.0410 | 0.5302 | 59.00 | 42.00 |
| 31 | 32 | 0.3510 | 0.1160 | 0.00 | 0.00 | 11 | 66 | 0.2012 | 0.0611 | 18.00 | 13.00 |
| 32 | 33 | 0.8390 | 0.2816 | 14.00 | 10.00 | 66 | 67 | 0.0470 | 0.0140 | 18.00 | 13.00 |
| 33 | 34 | 1.7080 | 0.5646 | 19.50 | 14.00 | 12 | 68 | 0.7394 | 0.2444 | 28.00 | 20.00 |
| 34 | 35 | 1.4740 | 0.4873 | 6.00 | 4.00 | 68 | 69 | 0.0047 | 0.0016 | 28.00 | 20.00 |

active and reactive power demand profiles while considering the average solar power availability [10]. The corresponding demand variations are depicted in Figure 4.

The objective function for the PV generation units was evaluated using the parameters listed in Table 4. Likewise, the cost-related information for the D-STATCOMs is summarized in Table 5.

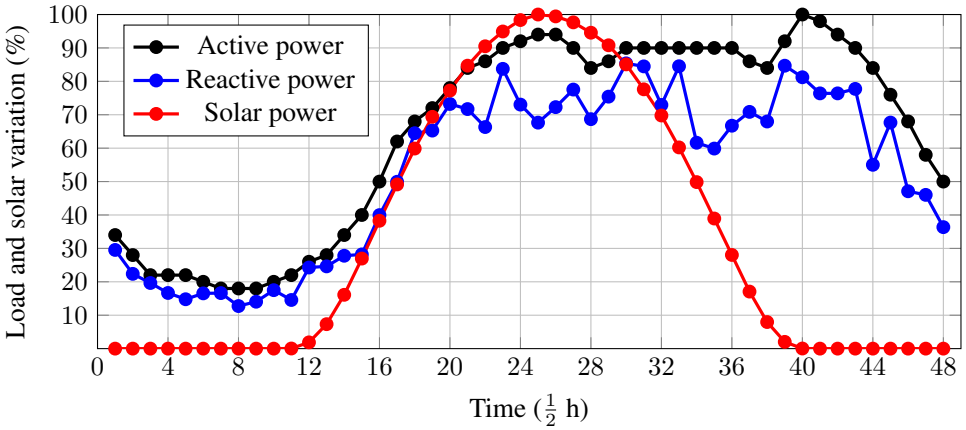


Figure 4. Daily power consumption and solar generation behavior

Table 4. Parameters related to the optimal location and capacity of PV systems in the studied distribution networks

| Parameter | Value | Unit | Parameter | Value | Unit |
|---|---|---|---|---|---|
| $C_{kWh}$ | 0.1390 | USD/kWh | $T$ | 365 | days |
| $t_a$ | 10 | % | $N_t$ | 20 | years |
| $\Delta h$ | 1 | h | $t_e$ | 2 | % |
| $C_{pv}$ | 1036.49 | USD/kWp | $C_{0andM}$ | 0.0019 | USD/kWh |
| $N_{pv}^{ava}$ | 3 | - | $p_i^{pv,\max}$ | 2400 | kW |
| $P_k^{pv,\min}$ | 0 | kW | | | |

Table 5. Objective function parameters $z$.

| Par. | Value | Unit | Par. | Value | Unit |
|---|---|---|---|---|---|
| $\omega_1$ | 0.30 | USD/Mvar$^3$ | $\omega_2$ | $-305.10$ | USD/Mvar$^2$ |
| $\omega_3$ | 127,380 | USD/Mvar | $\gamma$ | 1/20 | — |
| $Q_i^{comp,\min}$ | 0 | Mvar | $Q_{i,h}^{comp,\max}$ | 2000 | kvar |
| $P_i^{cg,\min}$ | 0 | W | $P_i^{cg,\max}$ | 5000 | kW |
| $Q_i^{cg,\min}$ | 0 | var | $Q_i^{cg,\max}$ | 5000 | kvar |

## 5. Numerical evaluation

The proposed master-slave optimization framework was computationally implemented using MATLAB (version 2024$a$). All experiments were carried out on a system equipped with an AMD Ryzen 7 3700 processor (2.3 GHz), 16 GB RAM, and a 64-bit version of Microsoft Windows 10 Single Language. Custom scripts were developed specifically for the ASOA and the successive approximations power flow method. To evaluate its performance, the proposed framework was compared against the VSA and the SCA described in [10] and [].

For the experimental setup, the PV sources were constrained to a maximum capacity of 2400 kW, while the D-STATCOM devices were limited to 2000 kvar. Each configuration allowed up to three PVs and three D-STATCOMs. The optimization algorithms used a population size of 50 individuals and ran for a maximum of 1000 iterations. Additionally, 100 independent runs were conducted for each method to ensure a robust statistical evaluation of the solution methodologies.

### *5.1. Numerical validations for the 33-bus grid*

Table 6 provides a comparative analysis of the optimization methods applied to the 33-bus distribution network. The results highlight the performance of the ASOA, the SCA, and the VSA in reducing project costs, identifying the optimal location of PV and D-STATCOM devices, and evaluating computational efficiency.

Table 6. Numerical results obtained in the 33-bus grid

| Scen. | $x_i^{comp}$ (Node) | $q_i^{comp}$ (Mvar) | $x_i^{pv}$ (Node) | $p_i^{pv}$ (MW) | $A_{\text{cost}_3}$ (USD) | Ave. time (s) |
|---|---|---|---|---|---|---|
| Benchmark case | — | — | — | — | 3,553,557.38 | — |
| VSA | [6, 15, 31] | [0.3801, 0.0640, 0.3543] | [9, 14, 31] | [0.9844, 0.6312, 1.7602] | 2,292,022.62 | 305.36 |
| SCA | [11, 12, 30] | [0.0092, 0.1143, 0.4617] | [7, 14, 31] | [0.4348, 1.8842, 1.0836] | 2,291,234.65 | 305.97 |
| ASOA | [13, 26, 30] | [0.1428, 0.1613, 0.3787] | [11, 16, 31] | [0.8269, 1.3512, 0.4736] | 2,290,519.25 | 311.85 |

A detailed analysis of the results reported in Table 6 is provided below:

i. The ASOA achieved the lowest total project cost, amounting to \$2,290,519.25, which represents a significant reduction of approximately 35.5429% in comparison with the benchmark case. This also demonstrates improved cost efficiency over the SCA (\$2,291,234.65) and VSA (\$2,292,022.62), with additional savings of \$715.40 and \$1,503.37. The results position the ASOA as the most effective method for minimizing costs within the 33-bus network.
ii. Regarding resource allocation, the ASOA selected buses 11, 16, and 31 for PV placement, assigning capacities of 826.9 kW, 1,351.2 kW, and 473.6 kW, respectively. For the D-STATCOMs, buses 13, 26, and 30 were identified as optimal, with corresponding reactive power allocations of 142.8 kvar, 161.3 kvar, and 378.7 kvar. Notably, the ASOA's node selections differ from those of the SCA and the VSA, showcasing its capacity to explore alternative configurations for improved system performance.
iii. In terms of computational efficiency, the ASOA reported an average runtime of 311.85 seconds. While this is slightly higher than the runtimes of the SCA (305.97 seconds) and the VSA (305.36 seconds), the marginal increase is justified by the superior cost savings achieved. Furthermore, the optimal solution provided by the ASOA indicates a requirement of approximately 560.0 kvar of reactive power and 3403.2 kWp of active power to achieve cost minimization. These values align closely with the power requirements identified by the SCA and the VSA, which demonstrates consistency across the methods.

To summarize, the ASOA not only delivers substantial cost reductions but also identifies strategic locations for PV and D-STATCOM devices while effectively balancing computational performance and optimization outcomes.

### *5.2. Numerical validations for the 69-bus grid*

A detailed comparison of the numerical results for the 69-bus network is presented in Table 7.

Table 7. Numerical results obtained in the 69-bus grid

| Scen. | $x_i^{comp}$ (Node) | $q_i^{comp}$ (Mvar) | $x_i^{pv}$ (Node) | $p_i^{pv}$ (MW) | $A_{\text{cost}_3}$ (USD) | Ave. time (s) |
|---|---|---|---|---|---|---|
| Benchmark case | — | — | — | — | 3,723,529.52 | — |
| VSA | [19, 53, 63] | [0.0871, 0.0075, 0.4555] | [15, 33, 62] | [0.8753, 0.5941, 2.0184] | 2,400,490.65 | 1680.10 |
| SCA | [7, 61, 65] | [0.0337, 0.3992, 0.1076] | [18, 59, 61] | [0.8761, 0.3407, 2.2949] | 2,396,720.37 | 1611.16 |
| ASOA | [16, 61, 64] | [0.0613, 0.4481, 0.0835] | [61, 62, 64] | [1.5558, 1.2796, 0.7524] | 2,395,320.95 | 1675.35 |

Considering the results reported in Table 7, the following can be stated:

- The cost reductions achieved by the optimization methods highlight the effectiveness of advanced algorithms in minimizing economic objectives for the 69-bus grid. The VSA achieves a total cost of \$2,400,490.65, which represents a 35.5318% reduction, while the SCA improves on this with a total cost of \$2,396,720.37, *i.e.*, a 35.6331% reduction. The ASOA exhibits the best performance, achieving a cost of \$2,395,320.95, representing a 35.6707% reduction. The ASOA outperforms the VSA and the SCA while offering additional savings of \$5,169.70 and \$1,399.42, which underscores its capability to optimize distribution network costs.
- The location and size of the PV systems differs across optimization methods, reflecting unique approaches to renewable energy integration. The ASOA allocates PV systems at buses 61, 62, and 64, with capacities of 1.5558 MW, 1.2796 MW, and 0.7524 MW, respectively. This allocation emphasizes a higher capacity at bus 61, likely leveraging its strategic advantage. In comparison, the SCA and the VSA allocate PV systems across other buses with varying distributions. The ASOA's targeted placement contributes to a superior performance by more effectively aligning generation capacity with network demand.

- Reactive power compensation is also handled differently by the optimization methods. The ASOA places D-STATCOMs at buses 16, 61, and 64, with reactive power capacities of 0.0613 Mvar, 0.4481 Mvar, and 0.0835 Mvar, respectively. This balanced distribution supports voltage regulation and power losses minimization. Conversely, the SCA concentrates reactive power compensation at bus 61 (0.3992 Mvar), while the VSA allocates the largest compensation at bus 63 (0.4555 Mvar). The ASOA's allocation strategy results in a more efficient and stable grid, reducing the project's overall costs.

Note that the ASOA stands out as the most effective optimization method for the 69-bus grid. It achieves the lowest costs while ensuring the optimal placement and sizing of the PV systems and D-STATCOMs to be installed. Its superior results demonstrate its potential as a robust solution for integrating renewable energy and enhancing the stability and efficiency of distribution networks.

## 6. Conclusions and future works

The Atan-Sinc Optimization Algorithm (ASOA) demonstrated exceptional performance in minimizing costs in both the 33-bus and the 69-bus networks. For the former, the ASOA achieved the lowest total project cost, *i.e.*, \$2,290,519.25, representing a significant reduction in comparison with the benchmark case and other methods. Similarly, in the 69-bus network, the ASOA yielded the best economic results, achieving a total cost of \$2,395,320.95, outperforming both the Sine-Cosine Algorithm (SCA) and the Vortex Search Algorithm (VSA) in terms of efficiency.

The ASOA effectively determined the optimal location and size of PV systems and D-STATCOM devices. In the 33-bus network, it allocated 3,403.2 kWp of PV capacity and 560.0 kvar of reactive power compensation. In the 69-bus system, it strategically distributed PV capacities of 1.5558 MW, 1.2796 MW, and 0.7524 MW across key buses while ensuring a balanced reactive power compensation. These results highlight the ASOA's capability to optimize resource allocation in line with network demands and operational constraints.

Although the ASOA required slightly higher computational times than the SCA and the VSA, it consistently delivered superior results across both medium- and large-scale test feeders. Its ability to handle mixed-integer nonlinear programming (MINLP) problems with complex constraints underscores its robustness and scalability, making it a reliable solution for real-world distribution grid optimization.

Future research could focus on the following directions. (i) Extending the model to include battery energy storage systems (BESS) alongside PV and D-STATCOM devices could further enhance grid flexibility and reliability, particularly during peak demand periods or when dealing with variable solar generation. (ii) Incorporating dynamic or stochastic load variations would improve the model's applicability to real-world scenarios, particularly for networks with a high penetration of intermittent renewable energy sources. (iii) Exploring hybrid optimization methods that combine the ASOA with other metaheuristic or deterministic algorithms could enhance convergence speed and solution quality. For instance, integrating the ASOA with machine learning-based predictive models could provide better initial solutions and guide the search process effectively in complex systems. (iv) Expand the application of the proposed ASOA approach to locate and integrate PVs and D-STATCOMs in large-scale distribution networks with hundreds of nodes.

ACKNOWLEDGEMENTS

The first author would like to thank Oficina de Investigaciones at Universidad Distrital Francisco José de Caldas for supporting the internal research project with code 33787724, titled "**Desarrollo de una metodología de gestión eficiente de potencia reactiva en sistemas de distribución de media tensión empleando modelos de programación no lineal**".

REFERENCES

1. Muhammad Bachtiar Nappu, Ardiaty Arief, and Willy Akbar Ajami. Energy Efficiency in Modern Power Systems Utilizing Advanced Incremental Particle Swarm Optimization–Based OPF. *Energies*, 16(4):1706, February 2023.

2. Fahad Bin Abdullah, Muhammad Arsalan Aqeeq, Rizwan Iqbal, Maria Abdullah, and Falak Shad Memon. Enhancing electricity distribution efficiency in Pakistan: A framework for progress and action. *Utilities Policy*, 88:101746, June 2024.
3. Xiangming Wu, Chenguang Yang, Guang Han, Zisong Ye, and Yinlong Hu. Energy Loss Reduction for Distribution Networks with Energy Storage Systems via Loss Sensitive Factor Method. *Energies*, 15(15):5453, July 2022.
4. Mustarum Musaruddin, Tambi Tambi, Waode Zulkaidah, Gamal Abdel Nasser Masikki, Agustinus Lolok, Abdul Djohar, and Marwan Marwan. Optimizing network reconfiguration to reduce power loss and improve the voltage profile in the distribution system: A practical case study. *e-Prime - Advances in Electrical Engineering, Electronics and Energy*, 8:100599, June 2024.
5. Oscar Danilo Montoya, Carlos Alberto Ramírez-Vanegas, and José Rodrigo González-Granada. Dynamic active and reactive power compensation in distribution networks using pv-statcoms: A tutorial using the julia software. *Results in Engineering*, 21:101876, March 2024.
6. Khaled Obaideen, Maryam Nooman AlMallahi, Abdul Hai Alami, Mohamad Ramadan, Mohammad Ali Abdelkareem, Nabila Shehata, and A.G. Olabi. On the contribution of solar energy to sustainable developments goals: Case study on mohammed bin rashid al maktoum solar park. *International Journal of Thermofluids*, 12:100123, November 2021.
7. Boutaina Talbi, Mounir Derri, Touria Haidi, and Abderrahmane Janyenne. Review of the Integration of Photovoltaic and Electric Vehicles on Distribution Network: Impacts and Enhancement Approaches. *Procedia Computer Science*, 236:93–100, 2024.
8. Sevda Jalali Milani and Gholamreza Nabi Bidhendi. Biogas and photovoltaic solar energy as renewable energy in wastewater treatment plants: A focus on energy recovery and greenhouse gas emission mitigation. *Water Science and Engineering*, 17(3):283–291, September 2024.
9. Nayeema Rashid and Md Humayun Kabir. Greenhouse Gas Emission Reduction through Electricity Generation from Solar Photovoltaic Systems: A Study in Dhaka. *The Dhaka University Journal of Earth and Environmental Sciences*, 12(1):1–8, January 2024.
10. Adriana Rincón-Miranda, Giselle Viviana Gantiva-Mora, and Oscar Danilo Montoya. Simultaneous integration of d-statcoms and pv sources in distribution networks to reduce annual investment and operating costs. *Computation*, 11(7):145, July 2023.
11. Oscar Danilo Montoya, Walter Gil-González, and Luis Fernando Grisales-Noreña. Optimal planning of photovoltaic and distribution static compensators in medium-voltage networks via the gndo approach. *Results in Engineering*, 23:102764, September 2024.
12. Alejandro Garcés-Ruiz. Power flow in unbalanced three-phase power distribution networks using matlab: Theory, analysis, and quasi-dynamic simulation. *Ingeniería*, 27(3):e19252, August 2022.
13. Saeed Rezaeian-Marjani, Sadjad Galvani, Vahid Talavat, and Mohammad Farhadi-Kangarlu. Optimal allocation of D-STATCOM in distribution networks including correlated renewable energy sources. *International Journal of Electrical Power & Energy Systems*, 122:106178, November 2020.
14. Abdullah M. Shaheen, Abdullah Alassaf, Ibrahim Alsaleh, and A.M. Elsayed. Enhanced kepler optimization for efficient penetration of pv sources integrated with statcom devices in power distribution systems. *Expert Systems with Applications*, 253:124333, November 2024.
15. Zedequias Machado Alves, Renata Mota Martins, Gustavo Marchesan, and Ghendy Cardoso Junior. Metaheuristic for the allocation and sizing of pv-statcoms for ancillary service provision. *Energies*, 16(1):424, December 2022.
16. Oscar Danilo Montoya, Carlos Alberto Ramírez-Vanegas, and Luis Fernando Grisales-Noreña. A Sine-Cosine Algorithm Approach for Optimal PV and D-STATCOM Integration in Distribution Systems. *Statistics, Optimization & Information Computing*, 13(3):1266–1279, November 2024.
17. Farzin Fardinfar and Mostafa Jafari Kermani Pour. Optimal placement of d-statcom and pv solar in distribution system using probabilistic load models. In *2023 10th Iranian Conference on Renewable Energy &; Distributed Generation (ICREDG)*. IEEE, March 2023.
18. Mezigebu Getinet Yenealem. Optimum Allocation of Microgrid and D-STATCOM in Radial Distribution System for Voltage Profile Enhancement Using Particle Swarm Optimization. *International Journal of Photoenergy*, 2024(1), January 2024.
19. Rajiv K. Varma and Ehsan M. Siavashi. Pv-statcom: A new smart inverter for voltage control in distribution systems. *IEEE Transactions on Sustainable Energy*, 9(4):1681–1691, October 2018.
20. Youssef Ait El Kadi, Fatima Zahra Baghli, and Yassine Lakhal. Pv-statcom in photovoltaic systems under variable solar radiation and variable unbalanced nonlinear loads. *International Journal of Electrical and Electronic Engineering &; Telecommunications*, pages 36–48, 2021.
21. Luis Fernando Grisales-Noreña, Daniel Sanin-Villa, and Oscar Danilo Montoya. Optimal integration of pv generators and d-statcoms into the electrical distribution system to reduce the annual investment and operational cost: A multiverse optimization algorithm and matrix power flow approach. *e-Prime - Advances in Electrical Engineering, Electronics and Energy*, 9:100747, September 2024.
22. L.F. Grisales-Noreña, J.C. Morales-Duran, S. Velez-Garcia, Oscar Danilo Montoya, and Walter Gil-González. Power flow methods used in AC distribution networks: An analysis of convergence and processing times in radial and meshed grid configurations. *Results in Engineering*, 17:100915, March 2023.
23. Abhisek Ukil, Vishal H Shah, and Bernhard Deck. Fast computation of arctangent functions for embedded applications: A comparative analysis. In *2011 IEEE International Symposium on Industrial Electronics*, pages 1206–1211. IEEE, June 2011.
24. B. A. Bailey and W. R. Madych. Cardinal sine series: Oversampling and non-existence. In *2015 International Conference on Sampling Theory and Applications (SampTA)*, pages 21–24. IEEE, May 2015.
25. Oscar Danilo Montoya, Walter Gil-González, Rubén Iván Bolaños, Diego Fernando Muñoz-Torres, Jesús C. Hernández, and Luis Fernando Grisales-Noreña. Effective power coordination of besus in distribution grids via the sine-cosine algorithm. In *2024 IEEE Green Technologies Conference (GreenTech)*. IEEE, April 2024.
26. Oscar Danilo Montoya, Edwin Rivas-Trujillo, and Luis Fernando Grisales-Noreña. Advanced Sech-Tanh Optimization Algorithm for Optimal Sizing and Placement of PV Systems and D-STATCOMs in Distribution Networks. *Statistics, Optimization & Information Computing*, 13(3):1–13, November 2024.